*R*esearch in
*A*stronomy and
*A*strophysics

# Optical spectroscopy and photometry of main-belt asteroids with a high orbital inclination

Aya Iwai[1], Yoichi Itoh[2], Tsuyoshi Terai[3], Ranjan Gupta[4], Asoke Sen[5] and Jun Takahashi[2]

[1] National Institute of Advanced Industrial Science and Technology, Ibaraki 305-8563, Japan

[2] Nishi-Harima Astronomical Observatory, Center for Astronomy, University of Hyogo, Hyogo 679-5313, Japan; *yitoh@nhao.jp*

[3] National Astronomical Observatory of Japan, Hilo, Hawaii 96720, USA

[4] Inter-University Centre for Astronomy and Astrophysics, Ganeshkhind, Pune 411 007, India

[5] Department of Physics, Assam University, Silchar 788 001, India

**Abstract** We carried out low-resolution optical spectroscopy of 51 main-belt asteroids, most of which have highly-inclined orbits. They are selected from D-type candidates in the SDSS-MOC 4 catalog. Using the University of Hawaii 2.2 m telescope and the Inter-University Centre for Astronomy and Astrophysics 2 m telescope in India, we determined the spectral types of 38 asteroids. Among them, eight asteroids were classified as D-type asteroids. Fractions of D-type asteroids are $3.0 \pm 1.1\%$ for low orbital inclination main-belt asteroids and $7.3 \pm 2.0\%$ for high orbital inclination main-belt asteroids. The results of our study indicate that some D-type asteroids were formed within the ecliptic region between the main belt and Jupiter, and were then perturbed by Jupiter.

**Key words:** minor planets, asteroids: general — techniques: spectroscopic

## 1 INTRODUCTION

Asteroids with a high orbital inclination are outliers. Terai & Itoh (2011) surveyed small asteroids at high ecliptic latitudes. By using wide and deep optical images taken with Suprime-Cam mounted on the Subaru Telescope, they detected 656 asteroids with high orbital inclinations. The orbital semi-major axes of most of these asteroids were derived to be between 2.0 astronomical units (AU) and 3.3 AU. Terai et al. (2013) found that the cumulative size distribution of high orbital inclination main-belt asteroids (hereafter MBAs) was shallower than that of low orbital inclination MBAs. It is generally believed that MBAs with high orbital inclinations have high collisional velocities. The shallow size distribution for high orbital inclination MBAs indicates that a large body has a higher disruptive strength when hypervelocity impacts occur.

The size distribution of high orbital inclination asteroids provides us with information regarding the process of planetesimal collision under different conditions compared to low orbital inclination planetesimals. However, the origin of high orbital inclination asteroids is still uncertain. Nagasawa et al. (2000) simulated the orbital evolution of asteroids. They included the depletion of gas in the solar nebula. An inner edge of the gas was moving outward at a velocity of $1 \times 10^{-5}$ AU yr$^{-1}$. Their study revealed that the eccentricity and inclination of the asteroids increased due to the motion of secular resonances caused by gas depletion, but the semi-major axis of the asteroids did not change. Ida & Makino (1993) investigated the orbital evolution of planetesimals near a protoplanet. Their numerical simulations showed that the planetesimals moved inward or outward with increasing orbital inclinations and/or eccentricities due to the gravitational perturbation of a protoplanet.

In this paper, we focus on D-type asteroids. D-type asteroids are abundant in the Trojan and main-belt population with a semi-major axis beyond $\simeq 3$ AU. Optical reflectance of D-type asteroids increases significantly with wavelength. Such optical reflectance and low albedo of D-type asteroids are similar to those of some comet nuclei. Many properties of D-type asteroids, including their spatial distribution and optical reflectance, have been dis-

cussed in the context of cometary evolution and asteroid populations. Detailed discussions on D-type asteroids are found, e.g., in Fitzsimmons et al. (1994).

We acquired low-resolution optical spectroscopy of MBAs. Most of these asteroids have highly-inclined orbits and optical colors consistent with spectral type D. A comparison of the number ratio for D-type asteroids in high and low inclination populations will help us to understand the formation and evolution process of high inclination asteroids. However, we cannot directly apply the D-type ratio from large volume photometric catalogs, e.g., the Sloan Digital Sky Survey - Moving Object Catalog 4 (SDSS-MOC 4) catalog, because classification using multi-color photometry is not certain (Carvano et al. 2010, DeMeo & Carry 2013, DeMeo & Carry 2014). Therefore, we carried out spectroscopic observations confirming D-type candidates and estimating the real D-type ratio. Hereafter, we define low orbital inclination MBAs as asteroids with a semi-major axis between 2.1 AU and 3.3 AU and with inclinations less than $10°$, and high orbital inclination MBAs as asteroids with the same semi-major axis range but with inclinations equal to or larger than $10°$.

## 2 OBSERVATIONS

We carried out low-resolution optical spectroscopy of MBAs using the Wide Field Grism Spectrograph 2 (WFGS2) mounted on the University of Hawaii (UH) 2.2 m telescope. The data were obtained on 2008 October 30 and 31 and 2011 October 19 and 20 with the low-dispersion grism 1 and a $1.4''$ width slit. These instrument settings achieved a wavelength coverage of 440–830 nm and a spectral resolution of $\sim$410 at 650 nm. Slit orientations were fixed in the north-south direction. The telescope was operated in non-sidereal tracking mode. The integration time for each object was between 180 s and 600 s. Facilities managed by the Inter-University Centre for Astronomy and Astrophysics (IUCAA) were also used. We employed the IUCAA Faint Object Spectrograph and Camera (IFOSC) mounted on the 2 m telescope at the IUCAA Girawali Observatory (IGO), India. The data were obtained on 2008 December 28 and 29 with the IFOSC 5 grism and a $1.5''$ width slit. The wavelength coverage was 520–1030 nm with a spectral resolution of $\sim$650 at 650 nm. Slit orientations were fixed in the north-south direction. The telescope was operated in non-sidereal tracking mode. The integration time for each object was between 300 s and 600 s.

Several criteria were used to select the targets. First, we selected asteroids with an orbital semi-major axis of between 2.1 AU and 3.3 AU, and with an orbital inclination greater than $10°$. We selected high orbital inclination asteroids because of the lack of high inclination samples in previous studies. One may postulate that the definition of high and low orbital inclination asteroids should be based on the $\nu_6$ resonance. Because the orbital inclination of the $\nu_6$ resonance varies with semi-major axis, classification based on the $\nu_6$ resonance may complicate the discussion on the selection bias of targets. Instead, we simply define high and low orbital inclination asteroids based on their inclinations. Most of the selected asteroids are listed in the SDSS-MOC 4 catalog and their optical magnitudes are given. We constructed an optical color-color diagram of the selected asteroids using the SDSS magnitudes, and classified those objects with $g-r \geq 0.5$ mag and $r-i \geq 0.2$ mag as candidates for D-type asteroids (Ivezić et al. 2001). Because we selected the targets on the $gri$ color-color diagram, we also considered the selection bias arising from the $gri$ color-color diagram (Sect. 4).

We were not able to completely fill the observing time while searching for D-type asteroids. Therefore, when we could not find any suitable candidates, we observed high orbital inclination asteroids instead, even if their SDSS colors were unknown. As a result, we observed a total of 48 high orbital inclination asteroids. We also observed three low orbital inclination asteroids for reference. The optical spectra of dwarfs with a spectral type of G were also taken as spectral standards.

After the observations for this work were carried out, DeMeo & Carry (2013) proposed a new method for the related taxonomy by using SDSS $g$-, $r$-, $i$- and $z$-band filters. They claimed that asteroid types can be identified with the $gri$ slope and $i - z$ color. D-type asteroids are classified as the group with the reddest $gri$ slope and the reddest $i - z$ color. The targets in this paper were classified into D-type, L-type or S-type with large $i - z$ magnitudes by applying the classification system of DeMeo & Carry (2013). Efficiency in the discovery of D-type asteroids would increase if we used the classification method of DeMeo & Carry (2013). This will be attempted in the future.

Additional photometric observations were carried out on 2012 November 7, 8 and 9 with the Multiband Imager for the Nayuta Telescope (MINT) mounted on the Nayuta Telescope at Nishi-Harima Observatory, Japan. We observed four asteroids whose SDSS magnitudes were unknown. We used SDSS $g-$, $r-$ and $i-$band filters. The field of view was $10' \times 10'$ with a pixel scale of $0.3''$. The full width at half maximum of the point spread functions was typically $2.0''$ or $2.5''$. The integration time was between 30 s and 600 s for each object. Since an as-

teroid rotates and its brightness may vary over time, we repeatedly observed a given asteroid in the $r$−band. The objects we investigated are summarized in Table 1.

We reduced the spectroscopic data with the following steps: overscan subtraction, bias subtraction, flat fielding, removal of scattered light caused by the telescope and/or the instrument, extraction of a spectrum and wavelength calibration. For the wavelength calibration, we used the O I and Na I lines measured from the sky for the UH data, and the emission lines from an Ne-Ar lamp for the IUCAA data. The spectra of the asteroids were then divided by the dwarf spectra. Thus, the spectra indicate the reflectivity of the asteroid. The spectrum of each asteroid was normalized to unity at 550 nm.

We reduced the photometric data with the following steps: overscan subtraction, bias subtraction and flat fielding with twilight flat frames. We used aperture photometry to measure the fluxes of the asteroids and several background stars in the same image. The aperture radius varied between 6 and 12 pixels, depending on the seeing size. Magnitudes of the asteroids were calculated using relative photometry compared to the background stars (SDSS DR9 catalog; Ahn et al. 2012). We used IRAF packages for all data processing.

## 3 RESULTS

Figure 1 shows the spectra of the asteroids and Table 2 lists their magnitudes and colors. The signal-to-noise ratios of the spectra in wavelengths between 660 nm and 740 nm ranged from 20 to 350 with a median value of 60.

Bus & Binzel (2002b) and Bus & Binzel (2002a) defined 26 asteroid spectral types. From the low-resolution optical spectra of thousands of asteroids, they calculated the average reflectivities of nine wavelength regions between 435 nm and 925 nm for each spectral type. We made template spectra of C-, S-, X-, D- and V-type asteroids by interpolating the average reflectivities for each asteroid spectral type. The template spectra were then normalized to unity at 550 nm. The template spectrum of a C-type asteroid is almost constant, whereas the spectra of S-type and V-type asteroids peak at approximately 700 nm. The template spectrum of an X-type asteroid increases gradually with wavelength, and that of a D-type asteroid increases significantly with wavelength. Individual asteroid spectra differ even if the asteroids are classified into the same spectral type. The standard deviation of the spectra among the same spectral type of asteroids is approximately 0.02. We calculated the residuals between the observed spectra and five template spectra. We then assigned a spectral type to an asteroid if

**Table 2** Magnitudes and Colors of the Asteroids

| Asteroid number | $g$-mag | $g − r$ [mag] | $r − i$ [mag] |
|---|---|---|---|
| 729 | 15.55±0.07 | 0.89±0.09 | 0.19±0.09 |
| 5222 | 16.54±0.04 | 0.75±0.10 | −0.04 ± 0.06 |
| 7290 | 17.40±0.05 | 0.54±0.07 | 0.17±0.07 |
| 94030 | 17.88±0.09 | 0.53±0.13 | 0.15±0.08 |

the residuals were at a minimum and were smaller than 0.07. As a result, we classified 38 asteroids; nine asteroids were classified as S-type, 16 as C-type, five as X-type, eight as D-type and none as V-type. Among them, the spectral types of six asteroids were previously assigned in Bus & Binzel (2002a) and the spectral type of one asteroid was assigned in Lazzaro et al. (2004). The spectral-type assignments in this work are consistent with the previous assignments for six out of seven assignments. Carvano et al. (2010) assigned spectral types for 63 468 asteroids based on SDSS photometric data. Among them, 22 019 asteroids have two or more observations. Of these, 14 962 show taxonomic variations. They employed nine classes for the spectral assignments, and found a transition between dissimilar classes, e.g., D to S, X to S, and C to S. They proposed extreme space weathering, contamination by metals, the coexistence of different mineralogies in the same body or phase reddening as the origin of these differences. We hypothesize that one inconsistent assignment between this work and the previous study may be attributed to inhomogeneity of the asteroid surface or ambiguity in the assignments.

## 4 DISCUSSION

We discuss the spatial distribution of D-type asteroids. D-type asteroids are abundant in the ecliptic plane between the main belt and the orbit of Jupiter ($\sim 50\%$, DeMeo & Carry 2013). The number of asteroids that have been categorized as spectral type D is too small for a statistical discussion on the spatial distribution of these asteroids. We used photometric data from the SDSS-MOC 4 catalog, as well as the results of spectroscopic studies (Bus & Binzel 2002a, Lazzaro et al. 2004, this work). Because the selection of our targets was based on the color-color diagram, we carefully combined the photometric studies and the spectroscopic studies to try to minimize selection bias. In the SDSS-MOC 4 catalog, 67 921 low orbital inclination MBAs are listed and 31 400 high orbital inclination MBAs are listed (Table 3). Ivezić et al. (2001) claimed that the SDSS $g−r$ and $r−i$ colors could be used to classify the spectral types of asteroids. We defined candidates for D-type asteroids as objects with $g − r \geq$

**Table 1** Targets and Assigned Spectral Type

| Asteroid number | *a* [AU] | *i* [°] | APmag[II] | UT Date | sec *z* | Ref. star (sec *z*) | Telescope | Spectral Type | |
|---|---|---|---|---|---|---|---|---|---|
| | | | | | | | | this work | previous work |
| 171 | 3.13 | 2.55 | 13.61 | 2008/10/31 | 1.07 | SAO 128811 (1.08) | UH | C | C[†] |
| 556 | 2.46 | 5.24 | 12.56 | 2008/10/31 | 1.03 | SAO 75211 (1.00) | UH | S | S[†] |
| 729 | 2.76 | 18.00 | 14.27 | 2011/10/20 | 1.07 | SAO 111802 (1.03) | UH | D | D[†] |
| 1241 | 3.19 | 23.55 | 14.53 | 2008/11/01 | 1.16 | SAO 109922 (1.04) | UH | C | |
| 1264 | 2.86 | 25.00 | 14.09 | 2008/12/28 | 1.66 | SAO 41806 (1.74) | IUCAA | C | C[†] |
| 1266 | 3.37 | 17.10 | 14.59 | 2011/10/20 | 1.03 | SAO 75098 (1.03) | UH | D | D[‡] |
| 1406 | 2.70 | 12.40 | 14.88 | 2011/10/21 | 1.09 | SAO 145806 (1.19) | UH | | Ld[†] |
| 2023 | 2.88 | 22.40 | 14.80 | 2011/10/21 | 1.15 | SAO 38934 (1.12) | UH | X | |
| 3139 | 3.20 | 20.53 | 15.52 | 2008/11/01 | 1.18 | SAO 73774 (1.30) | UH | C | C[‡] |
| 3346 | 3.19 | 21.50 | 15.60 | 2008/11/01 | 1.11 | SAO 109922 (1.04) | UH | C | |
| 4423 | 3.39 | 19.30 | 16.80 | 2008/11/01 | 1.26 | SAO 111908 (1.25) | UH | D | B[†] |
| 5222 | 2.77 | 34.58 | 15.69 | 2008/11/01 | 1.39 | SAO 111908 (1.25) | UH | C | |
| 5889 | 3.05 | 19.18 | 16.88 | 2008/11/01 | 1.12 | SAO 130080 (1.07) | UH | X | |
| 6052 | 3.24 | 21.70 | 15.88 | 2008/12/29 | 1.80 | SAO 115381 (1.32) | IUCAA | C | |
| 6148 | 2.28 | 22.70 | 17.77 | 2011/10/21 | 1.12 | SAO 145806 (1.19) | UH | | |
| 7290 | 2.56 | 24.76 | 15.13 | 2008/11/01 | 1.02 | SAO 109922 (1.04) | UH | C | |
| 7331 | 3.12 | 22.35 | 15.88 | 2008/10/31 | 1.08 | SAO 75211 (1.00) | UH | | |
| 8250 | 3.13 | 17.05 | 16.60 | 2008/11/01 | 1.10 | SAO 109922 (1.04) | UH | S | |
| 8882 | 2.36 | 23.10 | 16.24 | 2011/10/21 | 1.13 | SAO 145806 (1.19) | UH | D | |
| 13617 | 2.65 | 22.10 | 17.56 | 2011/10/21 | 1.23 | SAO 38934 (1.12) | UH | S | |
| 13810 | 3.15 | 17.04 | 16.81 | 2008/11/01 | 1.06 | SAO 130080 (1.07) | UH | D | |
| 15213 | 3.14 | 21.54 | 17.50 | 2008/10/31 | 1.11 | SAO 93158 (1.08) | UH | C | |
| 15410 | 3.11 | 17.15 | 16.91 | 2008/11/01 | 1.26 | SAO 111908 (1.25) | UH | C | |
| 15976 | 2.98 | 10.00 | 16.94 | 2011/10/20 | 1.03 | SAO 75098 (1.03) | UH | S | |
| 17435 | 2.37 | 22.10 | 17.58 | 2011/10/21 | 1.44 | SAO 130166 (1.52) | UH | | |
| 21552 | 2.60 | 22.10 | 17.34 | 2011/10/21 | 1.24 | SAO 130166 (1.52) | UH | | |
| 25572 | 2.59 | 22.90 | 17.00 | 2011/10/20 | 1.08 | SAO 111802 (1.03) | UH | S | |
| 25850 | 3.12 | 17.65 | 16.90 | 2008/11/01 | 1.10 | SAO 130080 (1.07) | UH | D | |
| 26571 | 2.79 | 15.20 | 17.47 | 2011/10/20 | 1.42 | SAO 75098 (1.03) | UH | | |
| 33750 | 2.80 | 32.70 | 17.15 | 2008/10/31 | 1.15 | SAO 128811 (1.08) | UH | C | |
| 37977 | 3.13 | 20.17 | 15.84 | 2011/10/21 | 1.11 | SAO 145806 (1.19) | UH | D | |
| 43142 | 2.59 | 14.40 | 16.13 | 2011/10/21 | 1.22 | SAO 147902 (1.27) | UH | S | |
| 43815 | 3.17 | 24.11 | 15.23 | 2008/11/01 | 1.08 | SAO 109922 (1.04) | UH | X | |
| 44215 | 2.58 | 12.40 | 17.22 | 2011/10/20 | 1.03 | SAO 75098 (1.03) | UH | | |
| 45411 | 2.63 | 12.10 | 16.56 | 2011/10/21 | 1.16 | SAO 38934 (1.12) | UH | S | |
| 46564 | 3.19 | 17.17 | 17.05 | 2008/10/31 | 1.12 | SAO 128811 (1.08) | UH | X | |
| 47334 | 2.63 | 13.80 | 16.28 | 2011/10/20 | 1.04 | SAO 75098 (1.03) | UH | | |
| 49591 | 3.22 | 17.68 | 16.40 | 2008/11/01 | 1.05 | SAO 109922 (1.04) | UH | C | |
| 54750 | 3.22 | 17.26 | 16.85 | 2008/11/01 | 1.25 | SAO 111908 (1.25) | UH | C | |
| 57036 | 2.34 | 23.80 | 17.76 | 2011/10/20 | 1.22 | SAO 111802 (1.27) | UH | S | |
| 64969 | 2.29 | 24.30 | 16.28 | 2011/10/21 | 1.30 | SAO 145806 (1.19) | UH | D | |
| 70104 | 3.17 | 22.95 | 16.70 | 2008/11/01 | 1.31 | SAO 111908 (1.25) | UH | S | |
| 73506 | 3.20 | 18.33 | 16.69 | 2008/10/31 | 1.10 | SAO 93158 (1.08) | UH | | |
| 93751 | 2.37 | 25.60 | 16.48 | 2011/10/21 | 1.37 | SAO 148719 (1.22) | UH | | |
| 94030 | 2.61 | 28.05 | 16.60 | 2008/10/31 | 1.06 | SAO 75211 (1.00) | UH | C | |
| 99202 | 3.20 | 22.24 | 17.02 | 2008/11/01 | 1.07 | SAO 130080 (1.07) | UH | C | |
| 163943 | 2.53 | 17.30 | 18.05 | 2011/10/21 | 1.21 | SAO 148719 (1.22) | UH | | |
| 193488 | 2.58 | 20.36 | 16.48 | 2008/11/01 | 1.11 | SAO 75874 (1.07) | UH | | |
| 198575 | 2.66 | 29.47 | 17.16 | 2008/10/31 | 1.03 | SAO 75211 (1.00) | UH | C | |
| 213177 | 2.38 | 24.20 | 17.80 | 2011/10/20 | 1.02 | SAO 75438 (1.00) | UH | | |
| 307783 | 3.09 | 17.73 | 16.54 | 2008/11/01 | 1.07 | SAO 109922 (1.04) | UH | X | |

Notes: [II] APmag is calculated on the JPL Small Body Database Browser. [†] Bus & Binzel (2002a). [‡] Lazzaro et al. (2004).
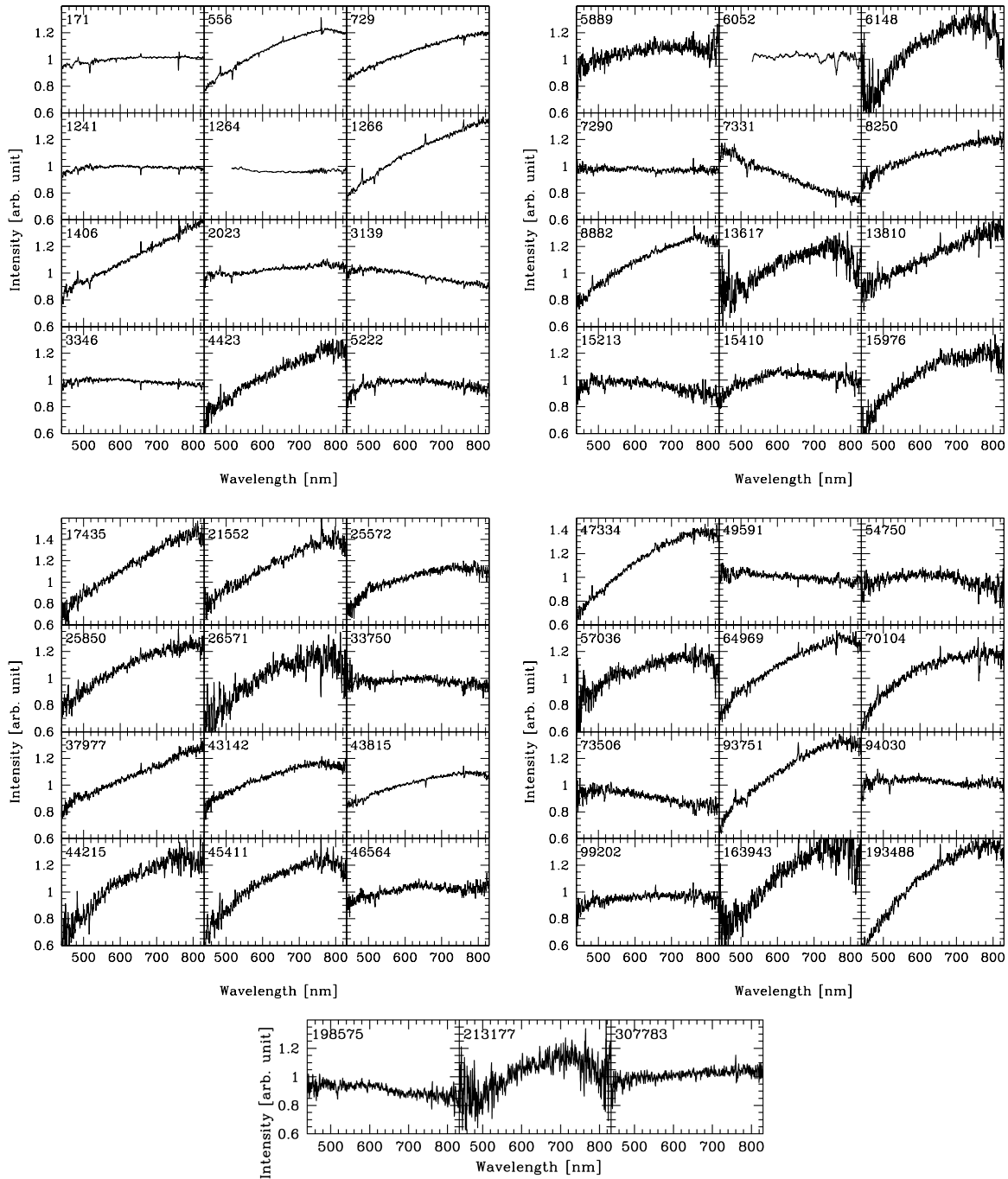
**Fig. 1** Optical spectra of the high orbital inclination asteroids. The reflectances are normalized to unity at 550 nm. Asteroids 171, 556 and 15123 are low orbital inclination asteroids. Spike patterns that appear in the spectra are artifacts due to telluric absorptions and photospheric absorptions of standard stars.

0.5 mag and $r - i \geq 0.2$ mag. A total of 26 261 low orbital inclination MBAs and 11 786 high orbital inclination MBAs have been identified as D-type candidates. Among them, optical spectra of 103 low orbital inclination candidates and 67 high orbital inclination candidates have been obtained (Bus & Binzel 2002a, Lazzaro et al.

2004, this work). Eight and 13 objects were spectroscopically assigned as D-type which are also low orbital inclination candidates and high orbital inclination candidates, respectively. We calculated the fraction of D-type asteroids. For low orbital inclination MBAs, the fraction of D-type asteroids is $(26261/67921) \cdot (8/103) =$
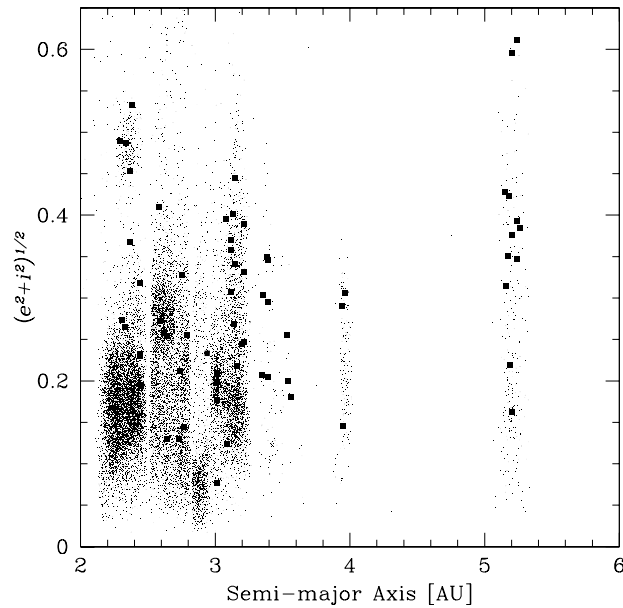
**Fig. 2** Distribution of asteroids. The vertical axis represents relative velocity of the asteroids. The *filled squares* indicate D-type asteroids and the *dots* indicate asteroids other than D-type. Data were compiled from Bus & Binzel (2002a), Lazzaro et al. (2004) and this work. D-type asteroids in the inner main-belt region do not have small relative velocity.

$3.0 \pm 1.1\%$. For high orbital inclination MBAs, the fraction is $(11786/31400) \cdot (13/67) = 7.3 \pm 2.0\%$. In this calculation, the uncertainty of the D-type fraction is controversial. The uncertainty involves ambiguity of taxonomy, accuracy of the orbital inclination and many other factors. We do not fully examine these factors. Instead, we simply regard the square root of the number of asteroids as the uncertainty associated with the number of asteroids. We conclude that the fraction of D-type asteroids is higher in the high orbital inclination MBAs than in the low orbital inclination MBAs. D-type asteroids are abundant in the ecliptic plane between the main belt and the orbit of Jupiter.

We propose that a number of D-type asteroids were formed near the ecliptic plane between the main belt and the orbit of Jupiter, and that some of the D-type asteroids then migrated inward via gravitational scattering by Jupiter and gained a high inclination orbit. One may investigate whether the D-type fraction changes if we apply the criteria for D-type candidates from DeMeo & Carry (2013) to our targets. However, we selected targets based on the $gri$ color-color diagram following Ivezić et al. (2001). Among our targets, only four asteroids match the D-type criteria of DeMeo & Carry (2013). This small sample prevents us from having a statistical discussion on the spatial distribution of the D-type asteroids. DeMeo & Carry (2013) deduced that the D-type mass ratio in the main-belt is ∼2%, or ∼4.4% if the four largest asteroids

are removed. The D-type number ratio in the main-belt derived in this work is ∼4%, if combining the high inclination and low inclination samples. This ratio seems consistent with DeMeo and Carry's result of 4.4% of mass in the main-belt belonging to D-type asteroids. However, DeMeo & Carry (2013) assumed that D-type asteroids have a bulk density of $1\,\mathrm{g\,cm^{-3}}$, roughly half the density of S- and C-type asteroids. Therefore, one may think that the number ratio of D-type asteroids should be ∼8%, which is higher than the result that this work presents. DeMeo & Carry (2013) calculated an average albedo of each asteroid type. We noticed that the albedo of the D-type asteroids is low among all types, especially in short wavelengths in the optical. This low reflectivity may cause the inconsistency between the number ratio and the mass ratio.

We consider the false-negative rate for identifying D-type asteroids using broadband photometry. For low orbital inclination asteroids in the SDSS MOC 4 catalog, 41 660 asteroids were not selected as D-type candidates, based on the color-color diagram. Among this sample, 3281 asteroids are actually classified as D-type asteroids, according to the classification of DeMeo & Carry (2013). Thus, the false-negative rate is $(3281/41660) = 7.9\%$, and the "true" D-type fraction of low orbital inclination asteroids is

$$(26261/67921)(8/103)+(41660/67921)\times 7.9\% = 7.8\%.$$

**Table 3** Fractions of the Asteroids in the SMASSII Catalog (Bus & Binzel 2002a)

| Inclination | Type | $2.1 < a \leq 2.5$ AU | $2.5 < a \leq 3.3$ AU |
|---|---|---|---|
| | C | $13.9 \pm 1.8\%$ | $38.2 \pm 2.4\%$ |
| $i < 10°$ | S | $62.3 \pm 3.8\%$ | $31.1 \pm 2.2\%$ |
| | D | $3.0 \pm 1.1\%$ | |
| | C | $15.3 \pm 3.4\%$ | $34.0 \pm 2.3\%$ |
| $i \geq 10°$ | S | $62.6 \pm 6.9\%$ | $24.0 \pm 2.0\%$ |
| | D | $7.3 \pm 2.0\%$ | |

In the same manner, the false-negative rate of high orbital inclination asteroids is $1752/(31400 - 11786) = 8.9\%$, and the "true" D-type fraction is

$$(11786/31400)(17/63) + (19614/31400) \times 8.9\% = 12.8\%.$$

The false-negative rates are high, which may effect the results. However, because the false-negative rates for low orbital inclination asteroids and high orbital inclination asteroids are similar, we think that the result of the higher D-type ratio in high orbital inclination asteroids still holds.

We next investigated the spatial distribution of C-type asteroids. C-type asteroids with a low orbital inclination are mainly distributed in the outer part of the main belt ($a > 2.5$ AU). If C-type asteroids were also perturbed by Jupiter, a fraction of the C-type asteroids should also have moved inward and acquired a high inclination. We calculated the fraction of C-type asteroids with a semi-major axis between 2.1 AU and 2.5 AU. The spectral classifications of Bus & Binzel (2002a) and Lazzaro et al. (2004) were used. Spectral types were assigned to 438 asteroids with a low orbital inclination and 131 asteroids with a high orbital inclination. Among them, 46 low orbital inclination asteroids and 20 high orbital inclination asteroids were classified as C-type asteroids. For simplicity, B-type asteroids were also classified as C-type. For low orbital inclination asteroids with a semi-major axis between 2.1 AU and 2.5 AU, the fraction of C-type asteroids is $(61/438) = 13.9 \pm 1.8\%$. For high orbital inclination asteroids with a semi-major axis between 2.1 AU and 2.5 AU, the fraction is $(20/131) = 15.3 \pm 3.4\%$. The origin of the difference in the fractions of C-type asteroids between low orbital inclination asteroids and high orbital inclination asteroids has not been identified.

We also calculated the fractions of S-type asteroids. For low orbital inclination asteroids with a semi-major axis between 2.1 AU and 2.5 AU, the fraction of S-type asteroids is $(273/438) = 62.3 \pm 3.8\%$. For high orbital inclination asteroids with a semi-major axis between 2.1 AU and 2.5 AU, the fraction of S-type asteroids

is $(82/131) = 62.6 \pm 6.9\%$. The difference between low orbital inclination asteroids and high orbital inclination asteroids has also not been identified for S-type asteroids. We consider that the orbits of asteroids located far from Jupiter have not been significantly perturbed by Jupiter.

Ida & Makino (1993) calculated the orbital evolution of planetesimals perturbed by a protoplanet. They indicated that planetesimals near the planet move such that they conserve Jacobi energy. The planetesimal's eccentricity and/or inclination increases once its semi-major axis increases or decreases. As a result, the planetesimals are distributed in a V-shape on the semi-major axis versus $(e^2 + i^2)^{1/2}$ (called the relative velocity) plane, with the apex of the V-shape located at the position of the protoplanet. The following studies extend numerical calculations of gravitational perturbation to the case of planetesimals with migrating planets (e.g. Gomes et al. 2005), or to the case of trans-Neptunian objects (e.g. Lykawka & Mukai 2008).

It is believed that a protoplanetary disk still contains a large amount of gas during the early stages of planetary formation. Adachi et al. (1976) calculated the accretion time of planetesimals. They found that the accretion time of a 10 km-sized planetesimal onto the Sun exceeds $10^9$ yr. The radii of the asteroids observed in this work are estimated to be several tens of kilometers, with an average radius of 30 km. Thus, we consider that gas drag in the protoplanetary disk did not significantly change the orbital semi-major axis of the asteroids.

Figure 2 shows the inclination and eccentricity of asteroids as a function of the orbital semi-major axis. The D-type asteroids show two distinct distributions. One is the asteroids with a semi-major axis of 5.2 AU. Those objects are called Trojan asteroids, which are resonant with Jupiter. Another distribution is the D-type asteroids in the inner main-belt but with high relative velocity. Carvano et al. (2010) classified asteroids based on the SDSS MOC 4 colors. They indicated that D-type asteroids are evenly distributed in the main-belt, but are not seen in the outer belt with inclinations greater than 20°. On the other hand, DeMeo & Carry (2013) and DeMeo & Carry (2014) found evidence for D-type asteroids in the inner- and mid-belts. Our result is consistent with the results of DeMeo & Carry (2013) and DeMeo & Carry (2014).

However, these results are not consistent with the influx of primitive material from Nice model like migration. For example, Levison et al. (2009) investigated orbital migration of trans-Neptunian objects. They focused on bodies with a size larger than 40 km and concluded that a significant fraction of objects in the main-belt are

captured primordial trans-Neptunian objects. They also found that the D-type and P-type material does not come closer than 2.6 AU. This result from numerical simulation is not consistent with findings based on observations in this work.

Walsh et al. (2011) proposed a dynamical model of the early Solar System, a so-called "Grand Tack" model. In this model, Jupiter first migrated inward by gas drag from the protoplanetary disk. When Jupiter reached ~1.5 AU from the Sun, Saturn grew to $60\ M_\oplus$, then migrated inward. At the same time, Jupiter tacked and migrated outward. As Jupiter moved, it initially scattered most of the planetesimals in the main-belt, but then re-populated the main-belt, where inner-belt asteroids originate between 1 and 3 AU and outer-belt asteroids between and beyond the giant planets. This distribution is consistent with the two separate populations of asteroids, if planetesimals from the inner disk are considered to be S-type and those from the outer regions C-type. The model indicates that both types of asteroids share similar distributions of eccentricity and inclination; most of the outer disk objects on planet-crossing orbits have high eccentricity, while many of the objects from between the giant planets were scattered earlier and damped to lower-eccentricity planet-crossing orbits. We identify D-type asteroids in the inner main-belt but with high relative velocity. Such a population was not predicted by Walsh et al. (2011).

Ida & Makino (1993) indicated that planetesimals were distributed in a V-shape with the apex at Jupiter in this diagram, if they were formed near Jupiter and were subsequently scattered. For D-type asteroids with a semi-major axis smaller than 5 AU, those asteroids with a smaller semi-major axis tend to have a large $(e^2 + i^2)^{1/2}$ value. This distribution of D-type asteroids might trace the left-side of the V-shaped structure. Further identification of D-type asteroids based on spectroscopic observations is required to confirm the gravitational perturbation of Jupiter on planetesimals.

## 5  CONCLUSIONS

We obtained low-resolution optical spectra of 51 asteroids. Most of these were MBAs with a high orbital inclination. We assigned spectral types to 38 asteroids. Eight asteroids were classified as D-type. We confirmed the existence of the inner main-belt D-type asteroids. We also found that the inner main-belt D-type asteroids have higher relative velocity.

(1)  For asteroids with a semi-major axis between 2.1 AU and 3.3 AU and with a high orbital inclination, the fraction of D-type asteroids was higher than that of asteroids with the same range of semi-major axis but with a low orbital inclination.

(2)  We compare the C- and S-type fractions of asteroids for the asteroids with a semi-major axis of between 2.1 AU and 2.5 AU and, between the asteroids with a high orbital inclination and the asteroids with a low orbital inclination, the fractions are comparable.

(3)  An abundant population of D-type MBAs with a high orbital inclination indicates that a fraction of high orbital inclination asteroids were formed near Jupiter and then migrated inward, resulting in a highly-inclined orbit.

## References

Adachi, I., Hayashi, C., & Nakazawa, K. 1976, Progress of Theoretical Physics, 56, 1756

Ahn, C. P., Alexandroff, R., Allende Prieto, C., et al. 2012, ApJS, 203, 21

Bus, S. J., & Binzel, R. P. 2002a, Icarus, 158, 146

Bus, S. J., & Binzel, R. P. 2002b, Icarus, 158, 106

Carvano, J. M., Hasselmann, P. H., Lazzaro, D., & Mothé-Diniz, T. 2010, A&A, 510, A43

DeMeo, F. E., & Carry, B. 2013, Icarus, 226, 723

DeMeo, F. E., & Carry, B. 2014, Nature, 505, 629

Fitzsimmons, A., Dahlgren, M., Lagerkvist, C.-I., Magnusson, P., & Williams, I. P. 1994, A&A, 282, 634

Gomes, R., Levison, H. F., Tsiganis, K., & Morbidelli, A. 2005, Nature, 435, 466

Ida, S., & Makino, J. 1993, Icarus, 106, 210

Ivezić, Ž., Tabachnik, S., Rafikov, R., et al. 2001, AJ, 122, 2749

Lazzaro, D., Angeli, C. A., Carvano, J. M., et al. 2004, Icarus, 172, 179

Levison, H. F., Bottke, W. F., Gounelle, M., et al. 2009, Nature, 460, 364

Lykawka, P. S., & Mukai, T. 2008, AJ, 135, 1161

Nagasawa, M., Tanaka, H., & Ida, S. 2000, AJ, 119, 1480

Terai, T., & Itoh, Y. 2011, PASJ, 63, 335

Terai, T., Takahashi, J., & Itoh, Y. 2013, AJ, 146, 111

Walsh, K. J., Morbidelli, A., Raymond, S. N., O'Brien, D. P., & Mandell, A. M. 2011, Nature, 475, 206